



Synthesis and evaluation of simple molecule as a co-adsorbent dye for highly efficient co-sensitized solar cells



Shengbo Zhu ^a, Zhongwei An ^{a,b,*}, Xiao Sun ^a, Zhisheng Wu ^b, Xinbing Chen ^a, Pei Chen ^a

^a Key Laboratory of Applied Surface and Colloid Chemistry, School of Materials Science and Engineering, Shaanxi Normal University, Xi'an, 710062, China

^b Xi'an Modern Chemistry Research Institute, Xi'an, 710065, China

ARTICLE INFO

Article history:

Received 6 February 2015

Accepted 1 April 2015

Available online 11 April 2015

Keywords:

Co-sensitized solar cells

Simple-structure dye

Co-adsorbent

Complementary absorption

Molecular size matching

Cyclic thiourea functionalization

ABSTRACT

One simple-structure dye and two bulky dyes have been designed for exploring a new co-sensitization system utilizing synergy between simple-structure and bulky organic dyes. This small-sized dye molecule can fill up the space defects between bulky dyes, and its strong absorption band from 350 to 500 nm can complement the absorption valleys of the bulky dyes. Additionally, the dye loading of titanium dioxide surface was investigated by Thermogravimetric analysis, which confirms that the molar loading of co-sensitized device has significantly increased. These results exhibit that the simple molecule can be used not only as a co-adsorbent to inhibit charge recombination and π - π aggregation between the bulky dyes but also as a co-sensitizer to improve light-harvesting ability.

© 2015 Elsevier Ltd. All rights reserved.

1. Introduction

With the growing severity of energy crisis and environment problem, scientists all over the world are beginning to turn their eyes to the exploitation of solar energy. As a promising light-harvesting device, dye-sensitized solar cells (DSSCs) have attracted widespread attention due to the features of friendly to environment, low carbon and easy fabrication [1–3]. In past decade, enormous efforts have been devoted toward improving the power conversion efficiency (PCE). To date, DSSCs based on metal-complex sensitizers have achieved the PCE of ~12% [4–6], and organic sensitizers also have reached the PCE of ~10% [7,8]. In recent years, however, organic sensitizers have received more and more attention because of their ease of syntheses, high molar extinction coefficients and simple preparation process in comparison with metal-complex sensitizers [9]. Researches on organic sensitizers mainly focus on molecular modification, especially donor and/or π -linker modification. These often give rise to large-sized and bulky dye molecules. Generally, additional groups are introduced into donors to avoid charge recombination and intermolecular aggregation [10–16]; electron-rich conjugation segments are inserted

into π -linkers to extend spectral response ranges [17–21]. Main advantages of these dyes lie in bigger conjugation system and broader absorption spectra. However, in addition to their tedious synthetic procedures, bulky molecular structures may decrease the amount of dye loading on TiO₂ surface. Therefore, developing simple-structure dyes as co-adsorbents will also be equally important. Recently, Han's group reported two simple-structure adsorbents used for co-sensitization with black dye which led to a superior PCE up to 11.4% [22]. Kim's group employed phenothiazine and phenoxazine as the donors to construct some simple dye molecules [23,24]. So far, improved conversion efficiencies have been successfully achieved in co-sensitized solar cells using organic dyes [18,25,26], or metal-complex and organic dye [27–33]. To the best of our knowledge, however, there are limited investigations available on simple organic molecules which serve as both co-adsorbents and complementary dyes used for co-sensitized solar cells.

In our previous studies [34–36], cyclic thiourea functionalized triphenylamine-based dyes exhibited significant photophysical and photovoltaic performances, including that: (i) such donor containing electron-rich nitrogen and sulfur heteroatoms in the cyclic thiourea group possesses high electron-donating ability [23]; (ii) broader and stronger spectral absorption in comparison with the corresponding triphenylamine-based dyes; (iii) the hexyl chains attached at the N-atom sites of cyclic thiourea groups can suppress the intermolecular aggregation and increase the solubility of dyes

* Corresponding author. Key Laboratory of Applied Surface and Colloid Chemistry, School of Materials Science and Engineering, Shaanxi Normal University, Xi'an, 710062, China.

E-mail address: gmeazw@163.com (Z. An).

[37–39]. However, the UV–Vis spectra of them are characterized by a “camelback” type, which leads to a weak absorption at around 400 nm. Besides that, there is another problem that we have to face: these tree-shaped dyes would leave large space between dye molecules when adsorbed on the TiO₂ surface. For these reasons, a novel simple molecule **SE** has been synthesized and evaluated. The results show that **SE** is not only a suitable co-adsorbent but also an effective dye in co-sensitization with dyes **AZ360** or **AZ362** (see Fig. 1 for the chemical structures), with following features: (i) this kind of non-triphenylamine dye inherits the cyclic thiourea group's superior bloodline but avoid the drawback of bulky molecular structures, which could be employed as fillers to fill up the space defects between bulky dyes; (ii) the hexyl chains introduced into **SE** molecule can inhibit intermolecular aggregation; (iii) the intense spectral response between 350 and 450 nm can complement the camelback-shaped spectra of **AZ360** and **AZ362** for achieving highly efficient light harvesting [27–30]. As expected, successful application of the simple-structure dye **SE** indicates the feasibility of this idea. Especially, the co-sensitized solar cell with **AZ362** + **SE** achieved the best complementary absorption and molecular size matching, and thus produced a PCE up to 7.65%, which increased by 9.29% in comparison with that of the DSSCs based on dye **AZ362** alone.

2. Experimental section

2.1. Synthesis and characterization

¹H NMR and ¹³C NMR spectra were recorded on Bruker AV-300 MHz or Bruker AV-400 MHz instruments with tetramethylsilane (TMS) as the internal standard. Gas chromatography mass spectra (GC-MS) were acquired in the electron ionization mode (EI) on Thermo DSQII. High resolution mass spectra (HRMS) were measured with a Bruker maXis mass spectrometer. Elemental analysis (C H N) was carried out on a VARIO-EL-III elemental analyzer.

All chemicals and solvents were purchased commercially and used without further purification unless otherwise stated. The synthetic details of **AZ360** are described in the Supporting Information. The synthetic details of **AZ362** were reported in our previous paper [36]. The synthesis of starting material **1** was reported in our previous paper [34], and the synthetic details of **SE** are described as follows:

1,3-dihexyl-5-iodo-1H-benzo[d]imidazole-2(3H)-thione (2). In a 100 mL 3-necked flask, compound **1** (8.6 g, 20.0 mmol), toluene (50 mL), and Lawesson reagent (6.5 g, 16.0 mmol) were added in turn under a nitrogen atmosphere. The reaction mixture was refluxed for 12 h. When cooling to room temperature, a yellow precipitate began to form and then was filtered. Following this, the filtrate was concentrated under reduced pressure and purified by column chromatography (PE/EA = 8/1, v/v; where PE is petroleum ether, boiling range: 60–90 °C; EA is ethyl acetate.) to give a yellow viscous liquid (6.6 g, 75% yield). ¹H NMR (300 MHz, CDCl₃): δ (ppm) 7.47 (s, 1H), 7.20 (d, *J* = 2.7 Hz, 1H), 6.94 (d, *J* = 8.1 Hz, 1H), 4.33–4.21

(m, 4H), 1.81–1.74 (m, 4H), 1.42–1.25 (m, 12H), 0.89–0.88 (m, 6H). ¹³C NMR (75 MHz, CDCl₃): δ (ppm) 169.62, 133.54, 132.09, 131.29, 117.59, 109.02, 85.32, 44.87, 44.83, 31.48, 31.44, 27.89, 27.79, 26.57, 26.51, 22.65, 22.53, 14.00, 13.92. GC-MS (EI, *m/z*) calcd. for (C₁₉H₂₉IN₂S): 444.11. Found: 444.18.

5-(1,3-dihexyl-2-thioxo-2,3-dihydro-1H-benzo[d]imidazol-5-yl)thiophene-2-carbaldehyde (3). In a 150 mL 3-necked flask, compound **2** (3.0 g, 6.8 mmol), 5-formyl-2-thiopheneboronic acid (1600 mg, 10.0 mmol), tetra-*n*-butylammonium bromide (TBAB) (660 mg, 2.1 mmol), N,N-dimethylformamide (DMF) (80 mL), Pd(PPh₃)₄ (115 mg, 0.1 mmol), H₂O (16 mL), and NaF (850 mg, 20 mmol) were added in turn under a nitrogen atmosphere. Following this, the reaction mixture was stirred for 5 h at 60 °C and then poured into EA. The organic layer was washed with water and dried over anhydrous MgSO₄. After removing the solvent, the crude product obtained was purified by column chromatography (PE/EA = 5/1, v/v) to give a yellow solid (940 mg, 32% yield). ¹H NMR (300 MHz, CDCl₃): δ (ppm) 9.82 (s, 1H), 7.69 (d, *J* = 3.0 Hz, 1H), 7.48 (d, *J* = 6.3 Hz, 1H), 7.33–7.32 (m, 2H), 7.15 (d, *J* = 6.3 Hz, 1H), 4.28–4.22 (m, 4H), 1.81–1.72 (m, 4H), 1.37–1.16 (m, 12H), 0.87–0.78 (m, 6H). ¹³C NMR (75 MHz, CDCl₃): δ (ppm) 182.61, 170.37, 154.03, 142.39, 137.41, 133.04, 132.78, 128.12, 123.98, 121.59, 109.40, 106.65, 44.99, 44.92, 31.52, 31.45, 27.89, 27.86, 26.64, 26.55, 22.53, 22.52, 14.19, 13.99. HRMS (ESI, *m/z*): [M+H]⁺ calcd. for (C₂₄H₃₃N₂OS₂): 429.2034, found: 429.2068.

(E)-2-cyano-3-(5-(1,3-dihexyl-2-thioxo-2,3-dihydro-1H-benzo[d]imidazol-5-yl)thiophen-2-yl)acrylic acid (SE). In a 100 mL 3-necked flask, compound **3** (940 mg, 2.2 mmol), acetic acid (50 mL), cyanoacetic acid (560 mg, 6.7 mmol) and ammonium acetate (560 mg, 7.3 mmol) were added in turn under a nitrogen atmosphere. The reaction mixture was refluxed for 5 h. After cooling to room temperature, the mixture was poured into ice water. The precipitate was filtered, washed by distilled water, and purified by column chromatography (PE/DCM = 5/1, v/v; where DCM is dichloromethane.) to give a red solid (650 mg, 59% yield). ¹H NMR (300 MHz, CDCl₃): δ (ppm) 8.34 (s, 1H), 7.79 (d, *J* = 1.8 Hz, 1H), 7.54 (d, *J* = 4.2 Hz, 1H), 7.42 (d, *J* = 1.8 Hz, 1H), 7.39 (s, 1H), 7.19 (d, *J* = 4.2 Hz, 1H), 4.32 (t, *J* = 3.9 Hz, 2H), 4.29 (t, *J* = 3.9 Hz, 2H), 1.86–1.79 (m, 4H), 1.46–1.31 (m, 12H), 0.89 (t, *J* = 3.3 Hz, 6H). ¹³C NMR (75 MHz, CDCl₃): δ (ppm) 170.49, 167.60, 155.54, 147.71, 140.18, 134.69, 133.35, 132.84, 127.60, 124.45, 121.86, 115.77, 109.44, 106.53, 90.62, 45.00, 44.91, 31.48, 31.44, 27.88, 27.87, 26.54, 26.51, 22.59, 22.53, 14.00, 13.99. HRMS (ESI, *m/z*): [M-H]⁻ calcd. for (C₂₇H₃₂N₃O₂S₂): 494.1936; found: 494.1938. Anal. calcd. for (C₂₇H₃₃N₃O₂S₂): C, 65.42; H, 6.71; N, 8.48. Found: C, 65.38; H, 6.73; N, 8.49.

2.2. Theoretical calculations

The electronic configuration and geometry structure of the dyes were optimized by density functional theory (DFT) calculations with the Gaussian 03 program package at the B3LYP/6-311G(d, p) level.

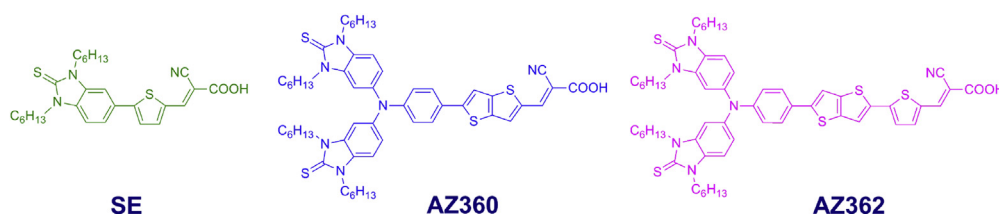


Fig. 1. Chemical structures of **SE**, **AZ360**, and **AZ362**. Herein C₆H₁₃ denotes *n*-hexyl.

2.3. UV–Vis absorption measurements

UV–Vis absorption spectra of the dyes in MeCN–DCM (1:1, v/v, where MeCN is acetonitrile; 1×10^{-5} M) solutions and on TiO₂ films (6.5 μm) were measured with a Shimadzu UV-3600 spectrophotometer.

2.4. Dye loading measurements

TiO₂ films (0.64 cm²) were prepared with a screen printing method according to the published method³⁵ and then immersed into a 0.4 mM dye bath in DCM solution under dark for 24 h at room temperature. Dye-loading properties of TiO₂ films were measured on Thermoanalyzer systems (Q1000DSC + LNCS + FACS Q600SDT) at a scanning rate of 10 °C min⁻¹ in the temperature range of 20–800 °C under an oxygen atmosphere. For co-sensitized TiO₂ films, the experimental procedures of desorption were conducted according to the published method [35]. The desorption solutions were measured with High performance liquid chromatography (HPLC, LC-20AT, Shimadzu Co., Japan); chromatography column: ODS (250 mm × 4.6 mm × 5 μm); detector: SPD-10A, λ = 235 nm; mobile phase: MeOH/MeCN/H₂O = 66.5/28.5/5.0 (containing 0.2% of triethylamine, where MeOH is methanol, v/v), 0.5 mL min⁻¹.

2.5. Device fabrication and photovoltaic measurements

The active area of the TiO₂ film was approximately 0.25 cm². All other fabrication processes of DSSCs were also performed according to the published method [35]. Photocurrent–voltage (*J*–*V*) characteristics of the DSSCs were measured under illumination with AM 1.5 G solar light from a 300 W xenon lamp solar simulator (94022A, Newport Co., USA). The incident light intensity was calibrated to 100 mW cm⁻² with a standard silicon solar cell. *J*–*V* characteristics were recorded with a digital source meter (Keithley 2400) controlled by a computer. The action spectra of monochromatic incident photon-to-current conversion efficiency (IPCE) for solar cells were tested on a commercial setup (QTest Station 2000 IPCE Measurement System, Crowntech, USA).

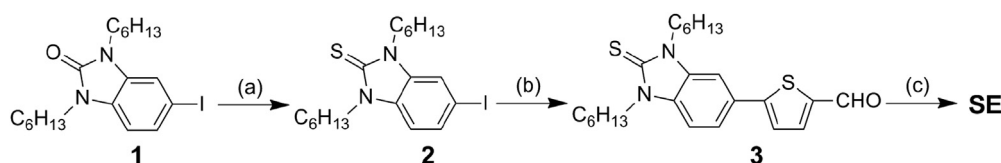
2.6. EIS measurements

Electrical impedance spectra (EIS) under dark with bias –0.7 V were also measured with CHI 660D Electrochemical Workstation at frequencies of 0.05–100,000 Hz. The magnitude of the alternative signal was 10 mV. Charge-transfer resistances were determined by fitting the impedance spectra using Z-view software.

3. Results and discussion

3.1. Design and synthesis

In our previous works [34–36], a series of cyclic thiourea functionalized triphenylamine-based dyes were synthesized. These dyes commonly consist of a bulky donor and a rod-like linker. It is



Scheme 1. Synthetic Route of **SE**. Reaction conditions: (a) Lawesson reagent, toluene, reflux, 12 h; (b) 5-formyl-2-thiopheneboronic acid, TBAB, DMF, Pd(PPh₃)₄, H₂O, NaF, 60 °C, 5 h; (c) cyanoacetic acid, CH₃COONH₄, CH₃COOH, reflux, 5 h.

Table 1

UV–Vis absorption and energy levels of by DFT calculations of **SE**, **AZ360**, and **AZ362**.

Dyes	$\lambda_{\text{abs}}/\text{nm}$ ($\epsilon/\text{M}^{-1} \text{cm}^{-1}$)		$E_{\text{HOMO}}/\text{eV}$	$E_{\text{LUMO}}/\text{eV}$	E_{g}/eV
SE	315 (19,700)	419 (39,400)	–5.78	–3.07	2.71
AZ360	332 (39,200)	465 (37,500)	–5.40	–3.07	2.33
AZ362	347 (34,700)	488 (37,800)	–5.24	–3.02	2.22

imaginable that these tree-shaped dyes would leave large space between molecules when adsorbed on the TiO₂ surface. For repairing the space defects, a novel simple-structure dye **SE** was designed. Compared with cyclic thiourea functionalized triphenylamine-based dyes, **SE** has a simple molecular structure and small volume. Such molecules can be employed as additional dyes to fill up the space defects between the tree-shaped dyes; on the other hand, hexyl chains attached at the cyclic thiourea group could suppress the intramolecular aggregation between the bulky dyes [22]. Furthermore, two cyclic thiourea functionalized triphenylamine-based dyes containing thienothiophene (**AZ360**) and thienothiophene-thiophene (**AZ362**) as π -linkers were synthesized for evaluating co-sensitization effectiveness.

As illustrated in Scheme 1, urea group at compound **1** was turned into thiourea group by Lawesson reagent. Suzuki coupling reaction between intermediate **2** and 5-formyl-2-thiopheneboronic acid was carried out using Pd(PPh₃)₄ as the catalyst to give compound **3**. Finally, the obtained compound **3** was converted to the target molecule **SE** via Knoevenagel condensation reaction with cyanoacetic acid in the presence of acetic acid and ammonium acetate. The synthesis of **AZ360** resembles the reported methods of similar dyes [35,36], and the details are described in the Supporting Information. The chemical structures of all target molecules were fully characterized by ¹H NMR, ¹³C NMR, and HRMS.

3.2. Theoretical calculations

Density functional theory (DFT) calculations were conducted to evaluate the geometries and electron distribution of the HOMO and LUMO energy levels of **SE**, **AZ360**, and **AZ362** (see Table 1). As shown in Fig. 2, the HOMO of **SE** is mainly distributed along the cyclic thiourea functionalized benzene ring and the thiophene unit, and the LUMO is delocalized across the thiophene unit and the acceptor. This means that electrons can successfully transfer from the cyclic thiourea functionalized benzene ring to the acceptor for the HOMO–LUMO transition. For **AZ360** and **AZ362**, the HOMOs and LUMOs perfectly revealed that the donor–acceptor character of the cyclic thiourea functionalized triphenylamine and the anchoring groups. The well-overlapped HOMO and LUMO orbitals on the π -linker indirectly suggest the well inductive or withdrawing electron tendency from the donor to the acceptor. Such dye architecture provides an energy gradient for the excitation and facilitates the HOMO to LUMO charge transfer transition, which is crucial to afford a favorable energetic pathway for electron injection into the conduction band of TiO₂ [40].

From a co-sensitization perspective, the superiority of simple-structure dye **SE** can be understood from the molecular structure.

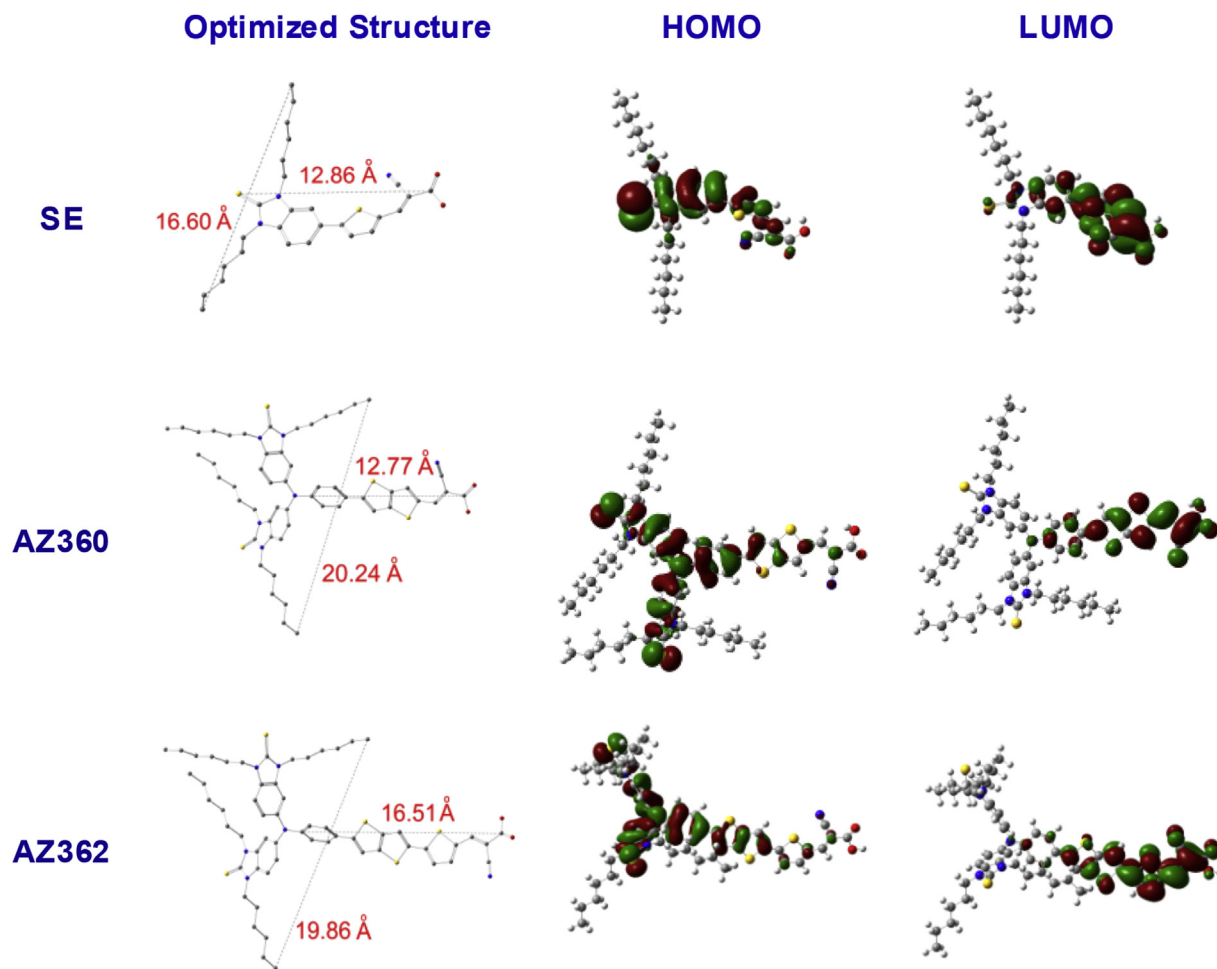


Fig. 2. The optimized structures and frontier orbitals of SE, AZ360, and AZ362 by DFT calculations.

Cyclic thiourea functionalized triphenylamine-based dye molecules, such as AZ360 or AZ362, possess a bulky donor along with a rod-like linker. In contrast, SE has a simple molecular structure and small volume, especially on the horizontal direction as observed in Fig. 2. The π -linkers' lengths of AZ360 and AZ362 are 12.77 and 16.51 Å, respectively. For SE, however, the length of the whole molecule is only 12.86 Å. Apparently, SE has a right shape and size to fill up the intermolecular space between the tree-shaped dye molecules when adsorbed on TiO₂ films. As seen from Fig. 3, the combination of SE and AZ362 seems to show a better molecular size matching in length.

3.3. Optical properties

As seen from Fig. 4a, SE presents a strong absorption band in the range of 350–500 nm along with a minor absorption peak at around 315 nm. The former may be ascribed to the intramolecular charge-transfer (ICT) transition between the cyclic thiourea functionalized benzene ring and the cyanoacetic acid acceptor moiety [41]; the latter might be assigned to the localized π - π^* transition of the cyclic thiourea functionalized benzene. The intensity of ICT transition is higher than that of the π - π^* transition (see Table 1). However, the absorption spectra of AZ360 and AZ362 exhibit two distinct broad absorption bands in the ranges of 300–400 nm and 400–600 nm, just like the other reported cyclic thiourea functionalized triphenylamine-based dyes [34–36]. It is obvious that there is an absorption valley at around 400 nm, in which, the absorption intensity is relatively weak. Fortunately, the strong

absorption band of SE can complement the absorption valley of AZ360 and AZ362, especially, the combination of SE and AZ362 seems to show more perfect complementary absorption. Hence, it is expected that the absorption defects of AZ360 and AZ362 will be complemented by addition of SE. Based on the above assumptions, different molar percentages of SE (10%, 30%, and 50%) were added into AZ360 and AZ362 for UV–Vis absorption measurements. As illustrated in Fig. 5a and c, the absorption valleys of AZ360 and AZ362 are well filled up; however, the absorption bands of AZ360 + SE and AZ362 + SE become narrow along with the

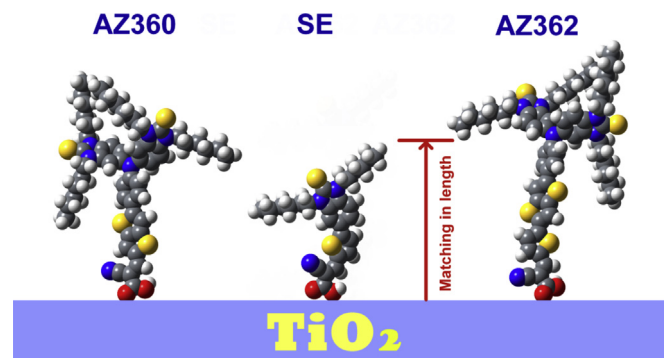


Fig. 3. Sketch map for molecular size matching of the dyes by DFT calculations.

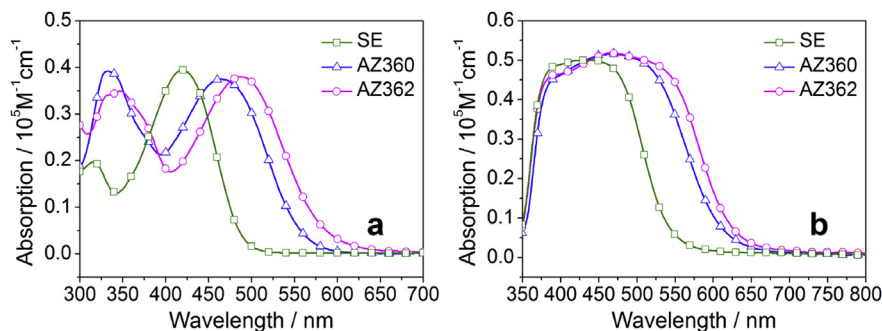


Fig. 4. UV–Vis absorption spectra of **SE**, **AZ360**, and **AZ362** in MeCN-DCM (1:1, v/v) solutions (a) and on TiO₂ films (b). The absorption of a TiO₂ film has been subtracted for clarity of presentation.

increasing addition amount of **SE**. This is easy to understand that the spectral response is gradually dominated by **SE**.

Compared with the results obtained in solutions, the absorption peaks of **SE**, **AZ360** and **AZ362** on TiO₂ films (Fig. 4b) are significantly broadened, implying that energy levels of the sensitizer molecules have somewhat changed due to the interaction with TiO₂ [42]. A closer look at the absorption spectra reveals that **SE** shows stronger absorption intensity in the range of 375–450 nm than **AZ360** and **AZ362**. This could be attributed to the powerful absorption ability of **SE** in this region. As seen from Fig. 5b and d, when co-adsorbed onto TiO₂ films, the absorption spectra of **AZ360** + **SE** and **AZ362** + **SE** are higher and broader than those of the corresponding individual dyes. This means that the addition of **SE** is favorable for improving the light-harvesting ability. Nevertheless, the absorption intensity of **AZ362** + **SE** changes more in the range of 375–450 nm in comparison with that of **AZ360** + **SE**, indicating that **SE** might be a more effective co-sensitizer for **AZ362**, which can be observed from Fig. 4a.

3.4. Dye loading properties

Dye loading was measured by Thermogravimetric analysis (TGA), and the results are listed in Table 2. (Additional data of TGA

are described in the Supporting Information, including Fig. S1 and Table S1). As shown in Fig. 6, all dyes adsorbed on TiO₂ surfaces were decomposed completely at around 550 °C, and they show similar decomposition behaviors. Weight percentages (*W*) of TiO₂ with **AZ360** + **SE** and **AZ362** + **SE** at 550 °C are 86.74% and 84.71%, respectively. After careful analysis, it is found that **AZ360** + **SE** exhibits less weight losses in comparison with **AZ360** (*W* = 86.11%), while **AZ362** + **SE** shows more weight losses in comparison with **AZ362** (*W* = 85.17%). These phenomena could be explained that there is competitive adsorption between **AZ360** and **SE** when co-adsorbed onto TiO₂ surface, thus more **AZ360** molecules were replaced by **SE** molecules; but filling effect may play a leading role between **AZ362** and **SE** due to suitable molecular sizes. HPLC analysis of the desorption solutions provide evidences that the dye-loading amounts (10^{-7} mol cm⁻²) of co-sensitized devices with **AZ360** + **SE** and **AZ362** + **SE** increase significantly in comparison with those of the devices with **AZ360** and **AZ362** alone (2.81 vs. 2.31 and 3.35 vs. 2.33, respectively).

3.5. Photovoltaic performance of DSSCs

The *J*–*V* curves of co-sensitized solar cells were measured under simulated AM 1.5G irradiation (100 mW cm⁻²), and the

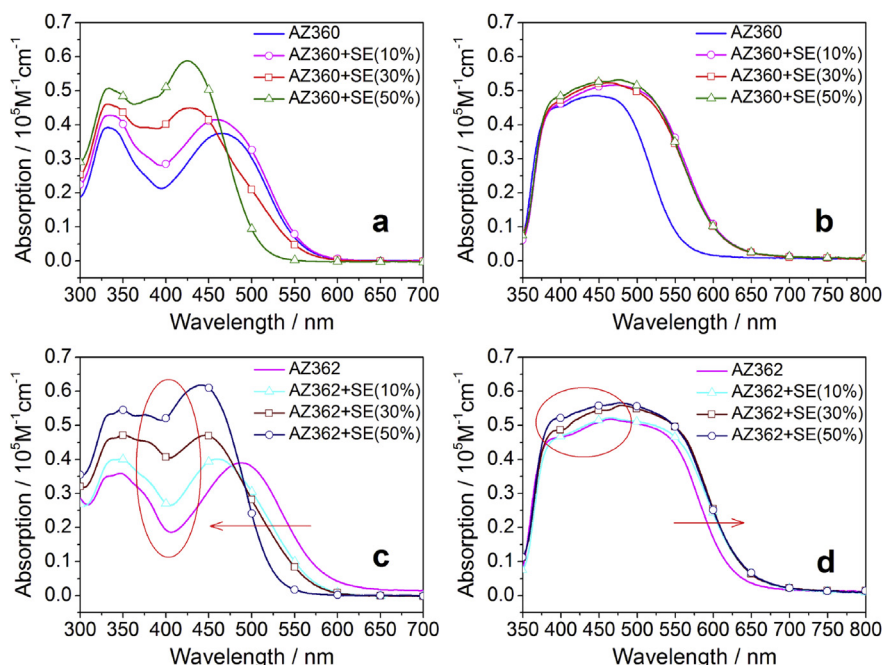


Fig. 5. UV–vis absorption spectra of different molar percentages of **SE** added to **AZ360** or **AZ362** in MeCN-DCM (1:1, v/v) solutions (a and c) and on TiO₂ films (b and d).

Table 2
Photovoltaic performance and dye-loading capacity for DSSCs based on SE, AZ360, AZ362, AZ360 + SE, and AZ362 + SE.

Dyes	$J_{sc}/\text{mA cm}^{-2}$	V_{oc}/mV	FF	PCE/%	IPCE/% (λ_{max}/nm)	Dye loading/ $10^{-7} \text{ mol cm}^{-2}$
SE	7.39	618.0	0.73	3.34	61.26 (410)	2.69
AZ360	14.92	680.1	0.65	6.60	73.23 (460)	2.31
AZ362	15.56	690.1	0.65	7.00	77.99 (490)	2.33
AZ360 + SE	15.16	690.0	0.67	7.03	75.96 (440)	2.81 (1.27 + 1.54)
AZ362 + SE	16.24	720.0	0.65	7.65	85.20 (440)	3.35 (1.63 + 1.72)

photovoltaic parameters are summarized in Table 2. To our surprise, the simple molecule SE yields a PCE of 3.34%, with a short-circuit current density (J_{sc}) of 7.39 mA cm^{-2} , an open-circuit voltage (V_{oc}) of 618.0 mV, and a fill factor (FF) of 0.73. The results suggest that utilizing this type of simple molecule as a co-sensitizer is feasible. For comparison, control groups sensitized by AZ360 or AZ362 were fabricated, which produce PCEs of 6.60% ($J_{sc} = 14.92 \text{ mA cm}^{-2}$, $V_{oc} = 680.1 \text{ mV}$, and $\text{FF} = 0.65$) and 7.00% ($J_{sc} = 15.56 \text{ mA cm}^{-2}$, $V_{oc} = 690.1 \text{ mV}$, and $\text{FF} = 0.65$), respectively.

Next, different molar percentages of SE (10%, 30%, and 50%) were added into AZ362 for optimizing co-sensitized conditions, and corresponding devices exhibit PCEs of 7.46% ($J_{sc} = 15.91 \text{ mA cm}^{-2}$, $V_{oc} = 700.0 \text{ mV}$), 7.65% ($J_{sc} = 16.24 \text{ mA cm}^{-2}$, $V_{oc} = 720.0 \text{ mV}$), and 7.26% ($J_{sc} = 14.97 \text{ mA cm}^{-2}$, $V_{oc} = 688.8 \text{ mV}$), respectively. (See Fig. S2 and Table S2)

Obviously, the addition of SE has a large impact on the photovoltaic performances of the co-sensitized devices. It is worth noting that, when 50% of SE was added, the J_{sc} and V_{oc} values decline significantly, thus resulting in a smaller PCE improvement. This might be due to competitive adsorption between the additional and main dyes [31,43]. As a result, the additional amount of SE should be controlled in 30%. Under the optimal conditions, co-sensitized solar cells based on AZ360 + SE or AZ362 + SE were fabricated. As seen from Table 2, the superiority of co-sensitization is obvious. Compared with AZ360 and AZ362, the PCEs of AZ360 + SE and AZ362 + SE are improved from 6.60% to 7.03% and from 7.00% to 7.65%, respectively. This should be caused by the improvement of J_{sc} and V_{oc} . The enhanced J_{sc} can be explained by the improved light harvesting due to complementary absorption [18], while the increased V_{oc} may be attributed to the intermolecular aggregation and charge recombination being suppressed by the insertion of co-adsorbent dye SE [22,38]. However, a closer look at Fig. 7a and c reveals that the addition of SE seems to be more effective for AZ362. This may be because that the simple-structure dye SE and tree-shaped dye AZ362 show the better complementary absorption (see Fig. 4a) and molecular size matching in length (see Fig. 3). The better complementary absorption is favorable for improving light harvesting, resulting in an increased photocurrent; at the same time, the suitable molecular size matching in length

could contribute to occupy the space defects between the tree-shaped dyes, thus inhibit the charge recombination and intermolecular aggregation.

To further understand effects of co-sensitization on the photo-current characteristics, the IPCE spectra were plotted as a function of excitation wavelength and are presented in Fig. 7b and d. The corresponding data are listed in Table 2. DSSCs based on SE, AZ360, and AZ362 display the maximum IPCE values of 61.26% at 410 nm, 73.23% at 460 nm, and 77.99% at 490 nm, respectively. After co-sensitization, the characteristic peaks of SE, AZ360, and AZ362 are clearly observed in the IPCE spectra of AZ360 + SE and AZ362 + SE, which suggest that two organic dyes were simultaneously adsorbed onto the TiO_2 surfaces [26]. Within the spectral region from 350 to 700 nm, the IPCE spectra of AZ360 + SE and AZ362 + SE are significantly improved in comparison with the corresponding individual dyes, and produce the maximum IPCE values of 75.96% at 440 nm and 85.20% at 440 nm, respectively, indicating that complementary absorption is an effective approach to extend the spectral response and enhance the photocurrent. From Fig. 7b and d, however, it can be seen that SE makes a greater contribution to AZ362 than that to AZ360, thus resulting in a higher maximum IPCE value. These results indirectly indicate that more SE were stuffed into the space defects between the tree-shaped dye AZ362 due to the better molecular size matching in length.

EIS measurements were performed to further elucidate the interfacial charge recombination process in co-sensitized solar cells. In the Nyquist plots (Fig. 8a), there are two semicircles, and the larger semicircle indicates charge-transfer resistance (R_{ct}) at the $\text{TiO}_2/\text{dye}/\text{electrolyte}$ interface, i.e., the recombination kinetics between conduction-band electrons in TiO_2 and I_3^- species from the electrolyte. A larger radius indicates a larger R_{ct} and slower electron recombination kinetics. Obviously, co-sensitized solar cells present the bigger R_{ct} and slower recombination than cells based on the individual dyes. These observations indicate that the “exposed” TiO_2 surfaces between dyes AZ360 or AZ362 may be covered by simple-structure dye SE, which are favorable for blocking I_3^- in contact with TiO_2 and reducing the back reaction probability [44,45]. In addition, the hexyl chains attached at SE could also impede the diffusion of I_3^- onto TiO_2 surfaces [28,46]. Therefore,

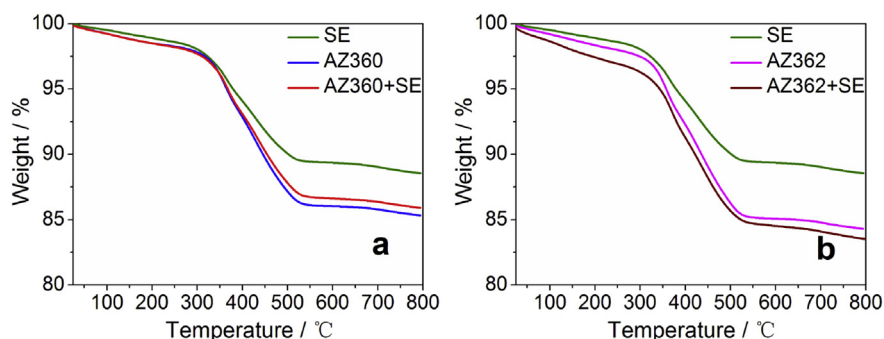


Fig. 6. TGA curves for TiO_2 adsorbed SE, AZ360, AZ362, AZ360 + SE, and AZ362 + SE.

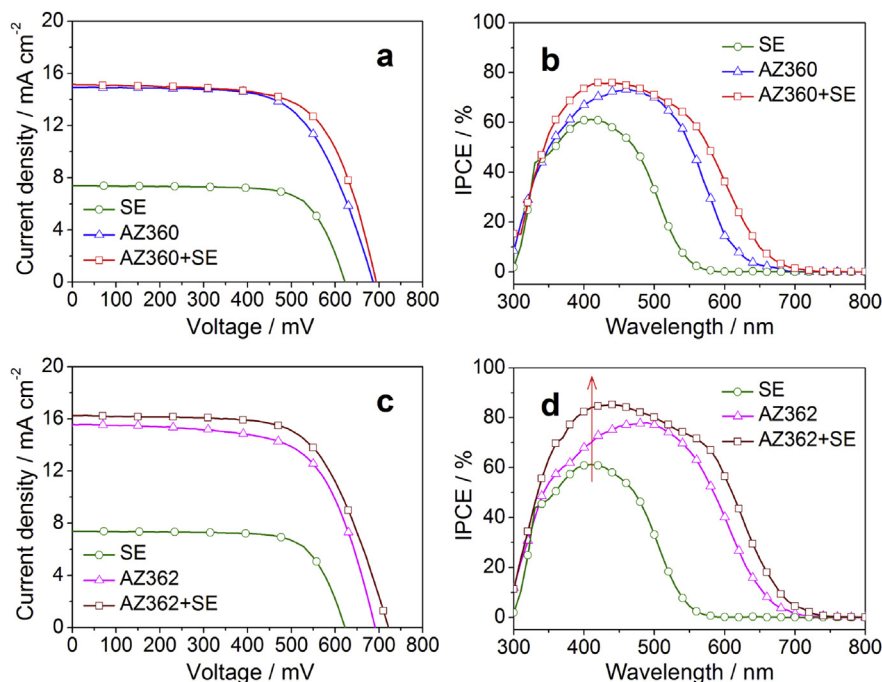


Fig. 7. J - V curves and IPCE spectra and for DSSCs based on SE, AZ360, AZ362, AZ360 + SE, and AZ362 + SE.

there should be higher electron density in the conduction band of TiO_2 that could cause a lift-up of the Fermi level for higher V_{oc} [30].

In the Bode phase plots (Fig. 8b), the lower-frequency peak is indicative of the charge-transfer process of injected electrons in TiO_2 . From the peak frequency, the electron lifetime (τ_e) can be calculated [15]. The calculated results increase in the order of SE (11.0 ms) < AZ360 (22.6 ms) < AZ362 (24.2 ms) < AZ360 + SE (24.5 ms) < AZ362 + SE (31.7 ms). Apparently, the co-sensitized solar cells based on AZ360 + SE and AZ362 + SE have longer electron lifetimes than those of the cells sensitized by AZ360 and AZ362 alone. This means much more effective suppression of the back reaction between the injected electrons and the electrolyte, thus resulting in the improvement of V_{oc} .

4. Conclusions

A novel simple-structure dye SE was synthesized and evaluated for co-sensitized solar cells. From DFT calculations, it can be seen that the cyclic thiourea functionalized benzene ring can be served

as an effective donor to construct dye molecule. The results suggest that this kind of simple-structure dye can not only complement the absorption valleys but also stuff the space defects of the bulky dyes, consequently resulting in improved light-harvesting abilities and enhanced photocurrent. On the other hand, the “exposed” TiO_2 surfaces between bulky dyes could be covered by co-adsorbent dye SE, which are favorable for blocking I_3^- in contact with TiO_2 and reducing the charge recombination rate. In addition, the hexyl chains introduced into SE molecule can inhibit intermolecular aggregation between bulky dyes, thus resulting in an enhanced V_{oc} of the co-sensitized devices. Under the optimal conditions, co-sensitized solar cell based on AZ362 + SE shows a PCE of 7.65%, which increases by 9.29% in comparison with that of DSSC based on AZ362 alone (PCE = 7.00%). This would spark our inspiration to design a series of new simple molecules used for both co-adsorbents and co-sensitizers, thereby form a new co-sensitization system with organic dyes, which is characterized by utilizing synergy between simple and bulky dyes to improve the photovoltaic performances of DSSCs.

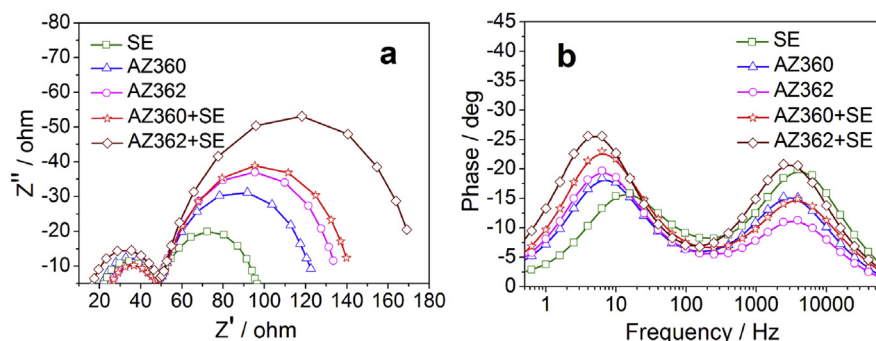


Fig. 8. EIS spectra for DSSCs based on SE, AZ360, AZ362, AZ360 + SE, and AZ362 + SE: Nyquist (a) and Bode phase plots (b).

Acknowledgments

This work was supported by the Natural Science Foundation of China (No. 51373092) and Fundamental Research Funds for the Central Universities (No. GK201304005) from the Department of Education. Our special thanks are also for the Fund of New Energy Devices and Materials provided by Mr. He Chong Ben, Hong Kong. We are grateful to Professor Wenliang Wang at Shaanxi Normal University for theoretical calculations. We also thank Minister Chao Gao and Miss Haimei Wu at Xi'an Modern Chemistry Research Institute for electrochemical measurements.

Appendix A. Supplementary data

Supplementary data related to this article can be found at <http://dx.doi.org/10.1016/j.dyepig.2015.04.003>.

References

- [1] O'Regan B, Grätzel M. A low-cost, high-efficiency solar cell based on dye-sensitized colloidal TiO₂ films. *Nature* 1991;353:737–40.
- [2] Grätzel M. Photoelectrochemical cells. *Nature* 2001;414:338–44.
- [3] Grätzel M. Recent advances in sensitized mesoscopic solar cells. *Acc Chem Res* 2009;42:1788–98.
- [4] Chen C-Y, Wang M, Li J-Y, Pootrakulchote N, Alibabaei L, Ngoc-le C-h, et al. Highly efficient light-harvesting ruthenium sensitizer for thin-film dye-sensitized solar cells. *ACS Nano* 2009;3:3103–9.
- [5] Gao F, Wang Y, Shi D, Zhang J, Wang M, Jing X, et al. Enhance the optical absorptivity of nanocrystalline TiO₂ film with high molar extinction coefficient ruthenium sensitizers for high performance dye-sensitized solar cells. *J Am Chem Soc* 2008;130:10720–8.
- [6] Yum J-H, Jung I, Baik C, Ko J, Nazeeruddin MK, Grätzel M. High efficient donor-acceptor ruthenium complex for dye-sensitized solar cell applications. *Energy Environ Sci* 2009;2:100–2.
- [7] Bai Y, Zhang J, Zhou D, Wang Y, Zhang M, Wang P. Engineering organic sensitizers for iodine-free dye-sensitized solar cells: red-shifted current response concomitant with attenuated charge recombination. *J Am Chem Soc* 2011;133:11442–5.
- [8] Zeng W, Cao Y, Bai Y, Wang Y, Shi Y, Zhang M, et al. Efficient dye-sensitized solar cells with an organic photosensitizer featuring orderly conjugated ethylenedioxythiophene and dithienosilole blocks. *Chem Mater* 2010;22:1915–25.
- [9] Wu W, Yang J, Hua J, Tang J, Zhang L, Long Y, et al. Efficient and stable dye-sensitized solar cells based on phenothiazine sensitizers with thiophene units. *J Mater Chem* 2010;20:1772–9.
- [10] Yang J, Ganesan P, Teuscher J, Moehl T, Kim YJ, Yi C, et al. Influence of the donor size in D- π -A organic dyes for dye-sensitized solar cells. *J Am Chem Soc* 2014;136:5722–30.
- [11] Urnikaitis S, Malinauskas T, Bruder I, Send R, Gaidelis V, Sens R, et al. Organic dyes with hydrazone moieties: a study of correlation between structure and performance in the solid-state dye-sensitized solar cells. *J Phys Chem C* 2014;118:7832–43.
- [12] Richard CA, Pan Z, Hsu HY, Cekli S, Schanze KS, Reynolds JR. Effect of isomerism and chain length on the electronic structure, photophysics, and sensitizer efficiency in quadrupolar (donor)₂-acceptor systems for application in dye-sensitized solar cells. *ACS Appl Mater Interfaces* 2014;6:5221–7.
- [13] Tan L-L, Xie L-J, Shen Y, Liu J-M, Xiao L-M, Kuang D-B, et al. Novel organic dyes incorporating a carbazole or dendritic 3,6-diiodocarbazole unit for efficient dye-sensitized solar cells. *Dyes Pigm* 2014;100:269–77.
- [14] Zhang J, Yang L, Zhang M, Wang P. Theoretical investigation of the donor group related electronic structure properties in push-pull organic sensitizers. *RSC Adv* 2013;3:6030–5.
- [15] Wan Z, Jia C, Duan Y, Zhou L, Lin Y, Shi Y. Phenothiazine-triphenylamine based organic dyes containing various conjugated linkers for efficient dye-sensitized solar cells. *J Mater Chem* 2012;22:25140–7.
- [16] Zong X, Liang M, Fan C, Tang K, Li G, Sun Z, et al. Design of truxene-based organic dyes for high-efficiency dye-sensitized solar cells employing cobalt redox shuttle. *J Phys Chem C* 2012;116:11241–50.
- [17] Zhang M, Zhang J, Fan Y, Yang L, Wang Y, Li R, et al. Judicious selection of a pinhole defect filler to generally enhance the performance of organic dye-sensitized solar cells. *Energy Environ Sci* 2013;6:2939–43.
- [18] Agosta R, Grisorio R, De Marco L, Romanazzi G, Suranna GP, Gigli G, et al. An engineered co-sensitization system for highly efficient dye solar cells. *Chem Commun* 2014;50:9451–3.
- [19] Pei K, Wu Y, Islam A, Zhu S, Han L, Geng Z, et al. Dye-sensitized solar cells based on quinoxaline dyes: effect of π -linker on absorption, energy levels, and photovoltaic performances. *J Phys Chem C* 2014;118:16552–61.
- [20] Wu Y, Zhu W. Organic sensitizers from D- π -A to D-A- π -A: effect of the internal electron-withdrawing units on molecular absorption, energy levels and photovoltaic performances. *Chem Soc Rev* 2013;42:2039–58.
- [21] Ni JS, You JH, Hung WI, Kao WS, Chou HH, Lin JT. Organic dyes incorporating the dithieno[3',2':3,4;2',3':5,6]benzo[1,2-c]furan moiety for dye-sensitized solar cells. *ACS Appl Mater Interfaces* 2014;6:22612–21.
- [22] Han L, Islam A, Chen H, Malapaka C, Chiranjeevi B, Zhang S, et al. High-efficiency dye-sensitized solar cell with a novel co-adsorbent. *Energy Environ Sci* 2012;5:6057–60.
- [23] Kim SH, Kim HW, Sakong C, Namgoong J, Park SW, Ko MJ, et al. Effect of five-membered heteroaromatic linkers to the performance of phenothiazine-based dye-sensitized solar cells. *Org Lett* 2011;13:5784–7.
- [24] Lee W, Yuk SB, Choi J, Kim HJ, Kim HW, Kim SH, et al. The effects of the number of anchoring groups and N-substitution on the performance of phenoxazine dyes in dye-sensitized solar cells. *Dyes Pigm* 2014;102:13–21.
- [25] Lu X, Lan T, Qin Z, Wang ZS, Zhou G. A near-infrared dithieno[2,3-a:3',2'-c]phenazine-based organic co-sensitizer for highly efficient and stable quasi-solid-state dye-sensitized solar cells. *ACS Appl Mater Interfaces* 2014;6:19308–17.
- [26] Kuang D, Walter P, Nüesch F, Kim S, Ko J, Comte P, et al. Co-sensitization of organic dyes for efficient liquid electrolyte-based dye-sensitized solar cells. *Langmuir* 2007;23:10906–9.
- [27] Sun X, Wang Y, Li X, Agren H, Zhu W, Tian H, et al. Cosensitizers for simultaneous filling up of both absorption valleys of porphyrins: a novel approach for developing efficient panchromatic dye-sensitized solar cells. *Chem Commun* 2014;50:15609–12.
- [28] Lan C-M, Wu H-P, Pan T-Y, Chang C-W, Chao W-S, Chen C-T, et al. Enhanced photovoltaic performance with co-sensitization of porphyrin and an organic dye in dye-sensitized solar cells. *Energy Environ Sci* 2012;5:6460–4.
- [29] Shrestha M, Si L, Chang C-W, He H, Sykes A, Lin C-Y, et al. Dual functionality of BODIPY chromophore in porphyrin-sensitized nanocrystalline solar cells. *J Phys Chem C* 2012;116:10451–60.
- [30] Chang S, Wang H, Hua Y, Li Q, Xiao X, Wong W-K, et al. Conformational engineering of co-sensitizers to retard back charge transfer for high-efficiency dye-sensitized solar cells. *J Mater Chem A* 2013;1:11553–8.
- [31] Shibayama N, Ozawa H, Abe M, Ooyama Y, Arakawa H. A new cosensitization method using the Lewis acid sites of a TiO₂ photoelectrode for dye-sensitized solar cells. *Chem Commun* 2014;50:6398–401.
- [32] Ozawa H, Shimizu R, Arakawa H. Significant improvement in the conversion efficiency of black-dye-based dye-sensitized solar cells by cosensitization with organic dye. *RSC Adv* 2012;2:3198–200.
- [33] Fan S-Q, Kim C, Fang B, Liao K-X, Yang G-J, Li C-J, et al. Improved efficiency of over 10% in dye-sensitized solar cells with a ruthenium complex and an organic dye heterogeneously positioning on a single TiO₂ electrode. *J Phys Chem C* 2011;115:7747–54.
- [34] Wu Z, An Z, Chen X, Chen P. Cyclic thiourea/urea functionalized triphenylamine-based dyes for high-performance dye-sensitized solar cells. *Org Lett* 2013;7:1456–9.
- [35] Zhu S, An Z, Chen X, Chen P, Liu Q. Approach to tune short-circuit current and open-circuit voltage of dye-sensitized solar cells: π -linker modification and photoanode selection. *RSC Adv* 2014;4:42252–9.
- [36] Zhu S, An Z, Chen X, Chen P, Liu Q. Cyclic thiourea functionalized dyes with binary π -linkers: Influence of different π -conjugation segments on the performance of dye-sensitized solar cells. *Dyes Pigm*, DOI: 10.1016/j.dyepig.2015.01.022.
- [37] Tian H, Yang X, Chen R, Hagfeldt A, Sun L. A metal-free “black dye” for panchromatic dye-sensitized solar cells. *Energy Environ Sci* 2009;2:674–7.
- [38] Koumura N, Wang Z-S, Mori S, Miyashita M, Suzuki E, Hara K. Alkyl-functionalized organic dyes for efficient molecular photovoltaics. *J Am Chem Soc* 2006;128:14256–7.
- [39] Chai Q, Li W, Wu Y, Pei K, Liu J, Geng Z, et al. Effect of a long alkyl group on cyclopentadiene as a conjugated bridge for D-A- π -A organic sensitizers: IPCE, electron diffusion length, and charge recombination. *ACS Appl Mater Interfaces* 2014;6:14621–30.
- [40] Katono M, Bessho T, Wielopolski M, Marszalek M, Moser J-E, Humphry-Baker R, et al. Influence of the anchoring modes on the electronic and photovoltaic properties of D- π -A dyes. *J Phys Chem C* 2012;116:16876–84.
- [41] Li W, Liu B, Wu Y, Zhu S, Zhang Q, Zhu W. Organic sensitizers incorporating 3,4-ethylenedioxythiophene as the conjugated bridge: joint photophysical and electrochemical analysis of photovoltaic performance. *Dyes Pigm* 2013;99:176–84.
- [42] Rakstys K, Solovjova J, Malinauskas T, Bruder I, Send R, Sackus A, et al. A structural study of 1-phenyl-1,2,3,4-tetrahydroquinoline-based dyes for solid-state DSSC applications. *Dyes Pigm* 2014;104:211–9.
- [43] Sayama K, Tsukagoshi S, Mori T, Hara K, Ohga Y, Shinpou A, et al. Efficient sensitization of nanocrystalline TiO₂ films with cyanine and merocyanine organic dyes. *Energy Mater Sol Cells* 2003;80:47–71.
- [44] Di Carlo G, Caramori S, Trifiletti V, Giannuzzi R, De Marco L, Pizzotti M, et al. Influence of porphyrinic structure on electron transfer processes at the electrolyte/dye/TiO₂ interface in PSSCs: a comparison between meso push-pull and β -pyrrolic architectures. *ACS Appl Mater Interfaces* 2014;6:15841–52.
- [45] Love JC, Estroff LA, Kriebel JK, Nuzzo RG, Whitesides GM. Self-assembled monolayers of thiolates on metals as a form of nanotechnology. *Chem Rev* 2005;105:1103–69.
- [46] Feldt SM, Gibson EA, Gabrielsson E, Sun L, Boschloo G, Hagfeldt A. Design of organic dyes and cobalt polypyridine redox mediators for high-efficiency dye-sensitized solar cells. *J Am Chem Soc* 2010;132:16714–24.